Optimizing the Spectrum and Energy Efficiency in Dynamic Licensed Shared Access Systems

Samuel O. Onidare, Osuolale A. Tiamiyu, Quadri R. Adebowale, Oluwaseun T. Ajayi, Kazeem B. Adewole and Adeseko A. Ayeni

Department of Telecommunication Science, University of Ilorin,
P.M.B 1515, Ilorin, Nigeria
onidare.so@unilorin.edu.ng

Abstract: In the licensed shared access (LSA) spectrum-sharing scheme, the protection of the incumbent leads to degradation in the licensee's spectrum and energy efficiency. In this paper, the optimization of these two performance metrics for an LSA vertical sharing between an airport incumbent and a mobile network licensee during the period when the LSA spectrum is not available, (i.e, the incumbent is active) is examined. Considering a restriction zone of a pre-defined radius, a power allocation scheme for joint optimization of the energy and spectrum efficiency during the period of the incumbent's occupation of the LSA band is formulated. Specifically, for the joint optimization of the spectrum and energy efficiency, the weighted sum approach to solve the ensuing multi-objective optimization problem is adopted. Furthermore, various critical operational parameters in conjunction with the two performance metrics were investigated. The results obtained show that, with the proper selection of cell radius, eNodeB transmit power and user number per cell, the proposed system can simultaneously achieve the trade-off objective of improved spectrum and energy efficiency.

Keywords: Licensed shared access (LSA), fifth generation (5G), energy efficiency, spectrum efficiency

1. Introduction

Today, every discussion in virtually all spheres of human lives and endeavours is centred on the sustainability paradigm. As a result, terms such as, environment friendly, green technologies, conservation biology, renewable energy, ecovillages, eco-municipalities, green building, and green computing are common place. In conformity with the global trend, the fifth generation (5G) wireless communications system can be appropriately termed the green communication generation (GCG). In fact, a key requirement of 5G includes, a hundred times (100x) energy efficiency [1] and/or ninety percent (90%) reduction in energy consumption [2] more than the fourth generation (4G) wireless communication standard. In the light of the existing facts and Figureures this requirement is not just a performance improvement/enhancement issue but a necessity.

Recent studies have shown that the energy consumption of the information and communication technology (ICT) sector is on the increase. For example, the study in [3] revealed that the ICT sector alone consumed 670 Terra Watt-hour (TWh) in 2007, and about 930 TWh in 2012, an average of 6.6% annual increase in the energy consumption. At this rate, the fraction of ICT to the global energy consumption is projected to increase from 8% in 2008 to 14% in 2020 [4]. This corresponds to an estimated 1.43 billion tonnes (Gt) carbon dioxide equivalent (CO2e) emissions in 2020, up from 0.53GtCO2e in 2002 which when combined with those of non-ICT has resulted in a faster than expected growth of greenhouse gas (GHG) emission [5].

Apart from the global warming concerns, continual growth of GHG emission, if unchecked is a threat to the global economy. It was estimated that 5^0C of global warming is equivalent to a reduction of welfare by approximately 5% of global GDP [6]. The impact of increased energy consumption on the operating expenditure of ICT service providers is another factor worthy of consideration. The estimate for the cost of operating electrical grid-connected base stations yearly is put at three thousand dollars ($3,000). Remote areas deployment of such base stations

Received: October 22nd, 2022. Accepted: August 29th, 2023
DOI: 10.15676/ijeei.2023.15.3.1

could cost ten times (10x) more since they run mostly on generators powered by diesel engine [7].

Furthermore, the improvement in battery power, has been found to be at a significant lower rate to the increase in energy consumption of ICT systems especially the wireless mobile broadband devices. The projected improvement in battery power put at five to ten percent compound annual growth rate (5-10%CAGR) is significantly lower than expected growth rate of energy consumption in microprocessors [8].

These challenges are further exacerbated by the direct relationship between energy consumption and the expected exponential growth in the demand and services accompanying the improvement of the wireless broadband technology. The mobile data growth rate alone (excluding fixed wireless access) was forecasted to be thirty-nine percent (39%) CAGR between the year 2017 and 2023 [9]. However, in reality, the same report shows that the actual growth between the first quarter of 2017 and 2018 was actually fifty-four percent (54%) CAGR while [10] shows an even higher rate of seventy-nine percent (79%) between the third quarter of 2017 and 2018. Similarly, [11] forecasted the annual global IP traffic to reach 3.3 Zettabytes by the year 2021.

Since 5G is expected to facilitate more diverse service, more user density (about 1 million devices/Km^2) with significantly higher data rates (about 100x user experienced data rate) and better spectrum efficiency (3x) more than the 4G [1], it is obvious that the trend in global broadband traffic will continue. In fact, the global mobile traffic is forecasted to grow ten -to-one hundred times (10-100x) from 2020 to 2030 [12]. The above facts coupled with the fact that the ICT is expected to be the driving force in the global quest for a low carbon society [5], implies that researches in energy efficiency (EE) will continue to be a main part of the discussion in the foreseeable future.

Increasing transmission bandwidth, improves EE but at the cost of degraded system spectrum efficiency (SE) [13]. However, the challenge of spectrum scarcity makes this an undesirable solution. Flexible spectrum management in the name of dynamic spectrum sharing (DSS) has been proposed to solve the 'spectrum scarcity' menace which has been found to be largely created by spectrum underutilization. The Licensed Shared Access (LSA), sharing between an incumbent (the exclusive owner of the spectrum) and a licensee, (a spectrum tenant licensed by the incumbent) is one of the several DSS schemes to address the problem of spectrum under-utilization [14], [15].

Consequently there have been several research work on the LSA. One group of research work validated the viability of the scheme by carrying out experimental field trials on live LTE test beds [16] – [22]. Another body of research work modelled the LSA operation using queueing theory and Markov process and analysed the system's performance using metrics such as service interruption and blocking probability, average number of connected users, service failure and mean bit rate [23] – [26]. The work in [27] proposed the LSA for the flexible spectrum management requirement of the `smart city' in the emerging 5G era. Similarly, the LSA is also considered as one of the candidate solution to unexpected network down time in public safety network during disaster outbreak and rescue operations [28].

A critical limitation of the LSA is the exclusion/restriction zone where licensee operation is expected to be suspended when incumbent is active. This amounts to a significant reduction in efficiency of the LSA since the coverage area of the exclusion/restriction zone is usually large. The proposed solution to this is a dynamic exclusion zone which suggests a reduced transmit power regime during incumbent occupation of the spectrum [29], [30]. Limiting the transmission power results in corresponding decrease in achievable network data rate and EE. In view of the earlier mentioned challenges of GHG emission, spectrum scarcity, expected high data traffic as well as key EE and SE 5G goals, this option is sub- optimal.

This paper is focused on jointly optimizing the LSA system's EE and SE during the limit transmit power regime. None of the previous works have investigated these key requirements of any 5G technology. The work in [31] shows that the SE and EE of a mobile network operator can be improved by implementing a horizontal LSA agreement between it and a micro cellular

network owned by another operator. However, theirs is an horizontal sharing scheme which shows that by offloading traffic from macro cell to micro cell, the EE and SE can be improved significantly. On the other hand, our work investigated the optimum system efficiency (EE and SE) of the licensee in a vertical LSA sharing scheme while the incumbent's interference threshold is not exceeded.

The main contributions of this paper are summarised in the following:

- An optimal power allocation technique for joint optimization of both EE and SE is proposed.
- The effect of various operational parameters (i.e, the number of channels in a LSA licensee cell, the cell radius and the adopted enodeB transmit power) on these two performance metrics were also examined.
- Furthermore, the effect of circuit power and importance of the weight on the joint optimization problem is investigated.
- Finally, by smartly setting network design and configuration goals to take advantage of the bounds and limits of the relationship between the investigated operational parameters and the two efficiency metrics, the viability of simultaneously maximizing the two conflicting objectives of EE and SE was established.

The rest of this paper is organised as follows. Section 2 presents the system model and mathematical formulation. In Section III, the joint optimization of EE and sum rate was modeled using the weighted sum method to convert the multi-objective optimization problem into a single objective optimization problem. This was then solved by fractional programming. Section IV, discusses the simulation results and analysis followed by Section V, which discusses the conclusion.

2. System Model

This work focus on the exclusion/restriction zone of the LSA framework, which could be about 25 km radius for an airport incumbent [29] or even as bad as excluding over sixty percent (60%) of the United States population if the incumbent's system is the Department of Defence Naval radar [32]. For this work, a circular area with a radius similar to the exclusion zone radius for an airport incumbent is considered. Furthermore, it is assumed that the LSA licensee, a mobile network operator (MNO), has multiple cells of radius R within the exclusion zone (figure. 1). The incumbent uses the spectrum specifically when the air traffic control (ATC) system is communicating with the aircraft(s). In this time period, the spectrum is referred to as busy or unavailable, otherwise, the spectrum is free, and available for the MNO unrestricted access.

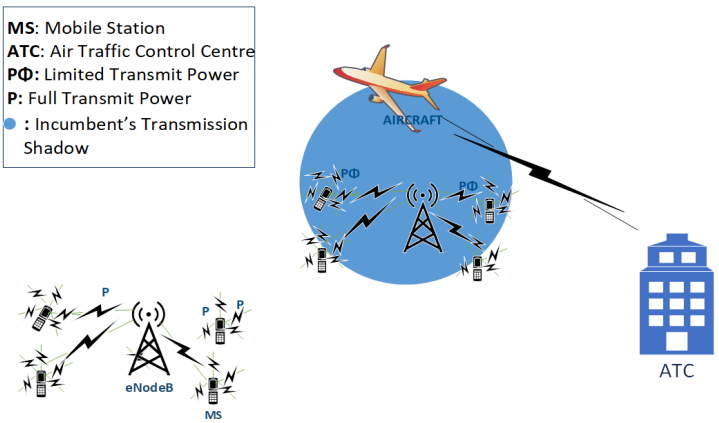

Figure 1. The system model: The limited tansmit power is only necessary at the region where incumbent's transmission shadow (blue shaded circle) intersects licensee cell.

The two systems, the ATC and the MNO ab-initio operates independently of one another. The MNO operates in the cellular band while the ATC uses the allocated spectrum for it. When the traffic load in the MNO system is below the installed capacity, its transmission is limited to its legacy spectrum, the cellular band. At this time instant, there is no interference consideration in the system model. However, when the required traffic in the MNO system exceeds the installed capacity, the MNO make use of the ATC spectrum under the LSA sharing scheme. When there is no transmission between the ATC tower and the aircrafts (landing or taking-off), the MNO now acting as the LSA licensee can make use of the spectrum unhindered and without interfering with incumbent owner (the ATC system). The interference consideration becomes a factor, when there is an active ATC transmission on the spectrum.

Figure 1 shows that, where the ATC transmission shadows intersects with the MNO transmission, there is a very strong possibility of both systems interfering with one another. In other regions of the exclusion/restriction zone, (i.e., where the transmitting systems shadow did not intersect) this possibility is significantly minimized or negligible. In the portion of the coverage area under consideration where the ATC transmission shadows intersects with the MNO transmission, there is need to protect the incumbent system from harmful interference from the MNO's transmission, hence the adoption of the limited transmit power policy [29].

B. The Licensee Interference

Here, the interference that could impair the ATC transmission to the flying aircraft during take-off or landing is considered. The eNodeB or base station antenna height is assumed to be sufficiently low relative to the ATC tower with a directional pattern, (directed downwards to the mobile stations), and as such the omni-directional transmissions of the mobile stations (MSs) become the main components of the interfering signal [29].

Considering the spatial distribution of the MSs in the cell as a Poisson point process,

$$\varphi = \{\rho_1, \rho_2, \ \ldots\ldots, \rho_{K.}\} \qquad (1)$$

the interference to a given aircraft located at a location, y in the vicinity of the cellular network is therefore:

$$I_\varphi(y) = \sum_{\rho\in\varphi} P_k h_k l(\|y - \rho\|), \qquad (2)$$

where, $l(\rho) = l\|\rho\|^{-\alpha}$, α is the path-loss exponent, h_k the fading coefficient which is an exponential random variable, P_k is the MS transmission power, l is the distance related power loss, and k denotes individual nodes or MSs randomly located in the cells of the LSA licensee.

Defining distance $\|y - \rho\|, \rho \in \varphi$, as $\|r\| \leq D$, the intervening area between them can then be represented as a ball $b(y, D)$ centred at y with a radius of D. Therefore, we can define an interference point process $\varphi_I = \varphi \cap b(y, D)$, (similar to the inner city model of the Cox process [33], where $\varphi_{I,}$ and φ are Poisson processes with density λ_I, and λ respectively, and $\lambda_I = \lambda c_d d r^{d-1}$, where, $c_d = \|b(0,1)\|$ is the volume of d-dimensional unit hyper ball.

Therefore the interference distribution from the MSs located within distance D to the position of the aircraft is [34], [35]:

$$f_I(i;\beta) = \frac{1}{\pi i}\sum_{k=1}^{\infty} \frac{\Gamma(\beta k+1)}{k!}\left(\frac{\lambda_I \pi \Gamma(1-\beta)}{i^\beta}\right)^k \sin k\pi(1-\beta) \qquad (3)$$

C. Spectrum Efficiency

In cases where the incumbent system is not utilizing its spectrum, the licensee is able to transmit at maximum power to guarantee the desired signal to noise and interference ratio (SINR) for each MS according to its QoS requirement.

Thus, the channels for k users is represented as a vector of random variables, $\boldsymbol{H} = [H_1, \ldots\ldots, H_K]^T$, and correspondingly the transmit-signal vector is $\boldsymbol{X} = [X_1, \ldots\ldots, X_K]$,. Therefore, the received signal power for K users, $\boldsymbol{P} = [P_1, \ldots\ldots, P_K]^T$, is $\boldsymbol{P} = \boldsymbol{XH} + \boldsymbol{Z}$, where $\boldsymbol{Z}$ is the additive white Gaussian noise vector, ($\boldsymbol{Z} = [Z_1, \ldots\ldots, Z_K]^T$). Furthermore, $H_k = \frac{G}{r_k^\alpha}$ (G, is

the propagation constant), and thus the total spectrum efficiency SE) is the summation of the achievable bit rate for each channel given by:.

$$SE = \sum_{k=1}^{K} \frac{1}{2} \log_2 \left(1 + \frac{X_K H_K + Z_K}{Z_K}\right). \quad (4)$$

D. Energy Efficiency

In order to achieve the energy efficiency (EE) target of 5G networks as well as achieving the expected high spectral efficiency, future system design must be able to either reduce energy consumption for each bit transmitted or/and equivalently maximize data transmitted per unit of energy expended. The energy dissipated is simply the sum of the circuit power and the transmission power scaled by the amplifier efficiency. Therefore EE is:

$$EE = \frac{\sum_{k=1}^{K} \frac{1}{2} \log_2 \left(1 + \frac{X_K H_K + Z_K}{Z_K}\right)}{P_{cr} + \frac{1}{\epsilon} \sum_{k=1}^{K} X_K H_K + Z_K} \quad (5)$$

where P_{cr} is the circuit power and ϵ is the amplifier efficiency.

3. Joint Optimization of Energy and Spectrum Efficiency

As earlier mentioned, two key performance metrics of the 5G era are high spectrum and energy efficiency (SE and EE). Achieving this in the context of LSA model is then translated into jointly maximizing the system spectrum and the energy efficiency; two conflicting objectives. The multi-objective optimization problem is thus formulated as:

$$\begin{aligned} &\max_{(P)} SE, \qquad \max_{(P)} EE, \\ &\text{s.t.} \quad \sum_{\rho \in \varphi} P_k h_k l(\|y - \rho\|) \leq I_{th}, \\ &P_k > 0, \qquad k = 1, \ldots\ldots\ldots\ldots, K \end{aligned} \quad (6)$$

where I_{th}, is the maximum interference the victim incumbent receiver can tolerate for proper operation.

The weighted sum method is adopted in order to convert the multi objective optimization problem (MOP) in (6) to a single objective optimization problem (SOP) by assigning weights to the objectives [36]. However, to ensure a consistent comparison between the two objectives, the following normalization is utilized:

$$\max_{(P)} \left[\frac{SE}{SE^{max}}\right], \qquad \max_{(P)} \left[\frac{EE}{EE^{max}}\right], \quad (7)$$

where SE^{max} and EE^{max} are defined such that $\boldsymbol{P}$ is the summation of the maximum transmit power not constrained by the interference threshold. Introducing the weight parameter (w), equation (6) becomes

$$\begin{aligned} &\max_{(P)} \quad w\left(\frac{SE}{SE^{max}}\right) + (1 - w)\left(\frac{EE}{EE^{max}}\right), \\ &\text{s.t.} \quad \sum_{\rho \in \varphi} P_k h_k l(\|y - \rho\|) \leq I_{th}, \\ &p_k > 0, \qquad k = 1, \ldots\ldots\ldots\ldots, K \end{aligned}$$

Given (5), equation (7) is transformed to:

$$\begin{aligned} &\max_{(P)} \quad w\left(\frac{SE}{wSE^{max} + (1-w)EE^{max} P_{tc}}\right), \\ &\text{s.t.} \quad \sum_{\rho \in \varphi} P_k h_k l(\|y - \rho\|) \leq I_{th}, \\ &P_k > 0, \qquad k = 1, \ldots\ldots\ldots\ldots, K, \end{aligned} \quad (8)$$

where $P_{tc} = P_{cr} + \frac{1}{\epsilon} \sum_{k=1}^{K} X_K H_K + Z_K$ is the total system consumed power.

Since SE, is proven to be convex, the above objective function as a ratio of a convex to an affine function is therefore, strictly quasi-convex and can be solved by fractional programming [37]. By the change of variable method, the transformation variable $t = [wSE^{max} + (1-w)EE^{max} P_{tc}]^{-1}$ is introduced an equivalent concave optimization problem is obtained:

$$\begin{aligned} &\max_{(P)} \quad t(SE) && 0 < w < 1, \\ &\text{s.t.} \quad t(wSE^{max} + (1-w)EE^{max} P_{tc}) = 1 \\ &\textstyle\sum_{\rho\in\varphi} P_k h_k l(\|y - \rho\|) \leq I_{th}, \\ &P_k > 0, \qquad k = 1, \ldots\ldots\ldots\ldots, K, \end{aligned} \tag{9}$$

The Lagrangian of (9) is:

$$\begin{aligned} &\mathcal{L}(P_k, u, \chi, \upsilon_k) \\ &= t(SE) + u[t(wSE^{max} + (1-w)EE^{max} P_{tc}) - 1] \\ &- \chi(\textstyle\sum_{k=1}^{K} P_k h_k l(\|y - \rho_k\|) - I_{th}) + \sum_{k=1}^{K} \upsilon_k P_k. \end{aligned} \tag{10}$$

The stationarity conditions for the Lagrangian in (10) are:

$$\frac{\partial \mathcal{L}(P_k,u,\chi,\upsilon_k)}{\partial P_k} = 0,$$

$$\frac{\partial \mathcal{L}(P_k,u,\chi,\upsilon_k)}{\partial t} = 0,$$

which are respectively found as:

$$\frac{t}{2\ln(2) Z_k \left(1+\frac{P_k}{Z_k}\right)} + ut\left[\frac{(1-w)EE^{max}}{\varepsilon}\right] - \chi[h_k l(\|y - \rho_k\|)] + \upsilon_k \tag{11}$$

and

$$SE + u[wSE^{max} + (1-w)EE^{max} P_{tc}] = 0. \tag{12}$$

Therefore, the optimal power allocation is

$$P_k^* = \frac{t\,\varepsilon}{2\ln(2)[\chi\phi_k - ut(1-w)]EE^{max}} - Z_k \tag{13}$$

4. Simulation Results and Analysis

In this section the simulation results of the LSA system are presented using the parameters shown in Table 1. The parameter values used in this work are obtained from such regularoty guidance as the ETSI operational parameter specifications [15], and as used in other literatures such as [26],[29],[30]. The nodes are assumed to be distributed in the eNodeB coverage areas of radius R according to radial density, $f_R(r)$,

$$f_R(r) = \begin{cases} \frac{2r}{D^2} & 0 \leq r \leq D, \\ 0 & otherwise. \end{cases} \tag{14}$$

Table 1. Simulation Parameters

Parameters	Value
eNodeB Radius	100 – 1000(m)
No of UEs	2, 5, 10, 20
Transmit Power	0.2-15.85(w) (or 23-42dBm)
Bandwidth	10MHz
Noise Density	-60dBm
Circuit Power	1(w)
Amplifier Efficiency	38%

Firstly, the analysis the EE of the system during the busy and idle spectrum period is done. Two observations can be made between the optimization of the system EE in the first and the non optimized system in the second sub plot of figure. 2. As a result of having to operate under a limited transmit power regime during the period the incumbent is active on its spectrum, the systems SE and hence the EE is reduced compared to the cases when the spectrum is free of incumbents activity (third sub plot of figure. 2.) However, optimizing the system significantly improve EE to values comparable with the cases where the licensee is operating at full transmit power. The second observation is the shape of the slope of the two graphs. With increasing transmission power, the optimized system's EE falls at a lower rate (approximately linear) compared with the exponential decrease in non-optimized system.

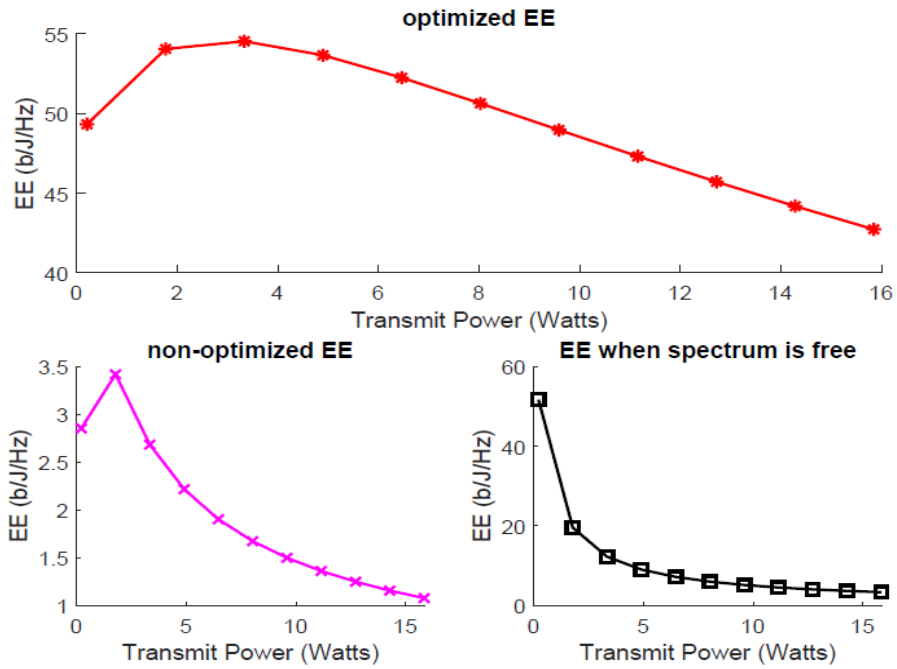

Figure 2. EE versus Transmit Power during busy and idle spectrum period.

Another interesting observation of the LSA's EE during period of incumbent's occupation of the spectrum is shown in the second and third sub plot of figure. 2. The EE versus transmit power curve is expected to be a monotonically decreasing function. However, when the spectrum is busy, even in the non-optimized case, the EE first increases before it decreases at a much lower rate than the usual. This can be explained by the fact that EE, as a ratio of SE to power consumed, can be increased by either increasing the SE and/or lowering the systems power consumption. Since, the LSA system operates under a limited power regime during busy spectrum period, the reduction in transmit power invariably translates to an increase in the system's EE at lower transmit power, hence making the EE vs power curve to deviate from the expected as shown in the sub-plot for when the spectrum is free.

Figure 3 shows the improvement in SE obtained using the proposed power allocation. As shown in the graph, the relative improvement gradually decreases with increased transmit power. When the eNodeB transmit power is set to 0.2watts, the increase is about ten times more than the non-optimized system, while at 15.85watts transmit power, the increase is just about twice. This can be explained by the fact that the Shannon capacity theorem has a cap on the transmit power at which increase in transmit power does not lead to a corresponding increase in the system SE.

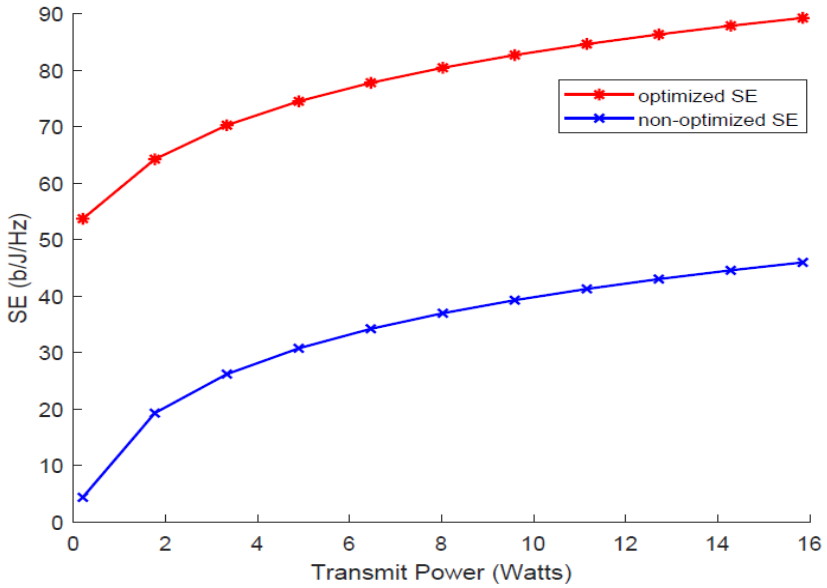

Figure 3. Comparison of the optimized and non-optimized system SE.

A. Effect of System Engineering Parameters on the SE and EE

Figure 4 shows the SE and EE behaviour of the joint SE and EE optimal power allocation of the LSA system during incumbent's occupation of the spectrum. Expectedly, the SE increases logarithmically with increase in transmission power. However, for the EE, there is an initial increase (peak at around 3watts mark) and then the expected decrease with increase in transmit power. The implication of this is that at a low transmit power, it is possible to simultaneously increase both the EE and the SE, instead of having to trade one off for the other.

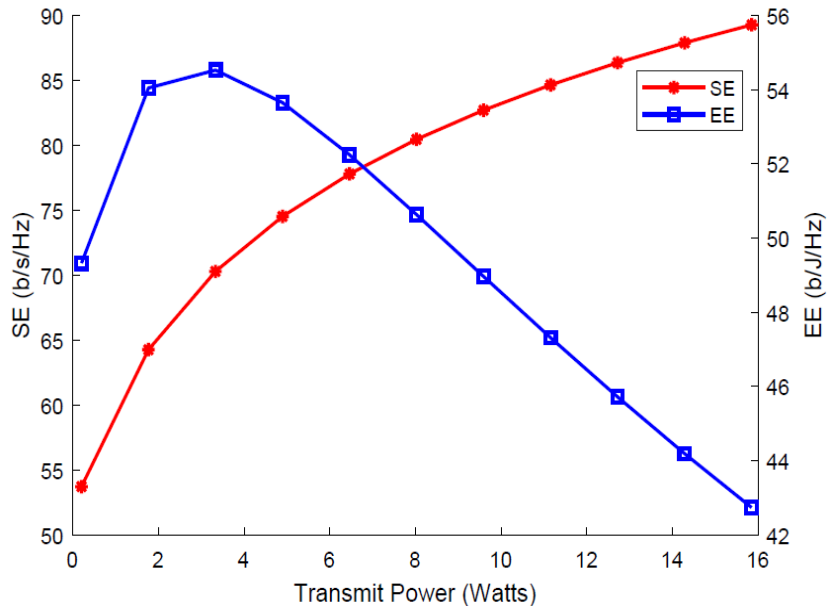

Figure 4. SE and EE versus transmit power.@ R=1000m

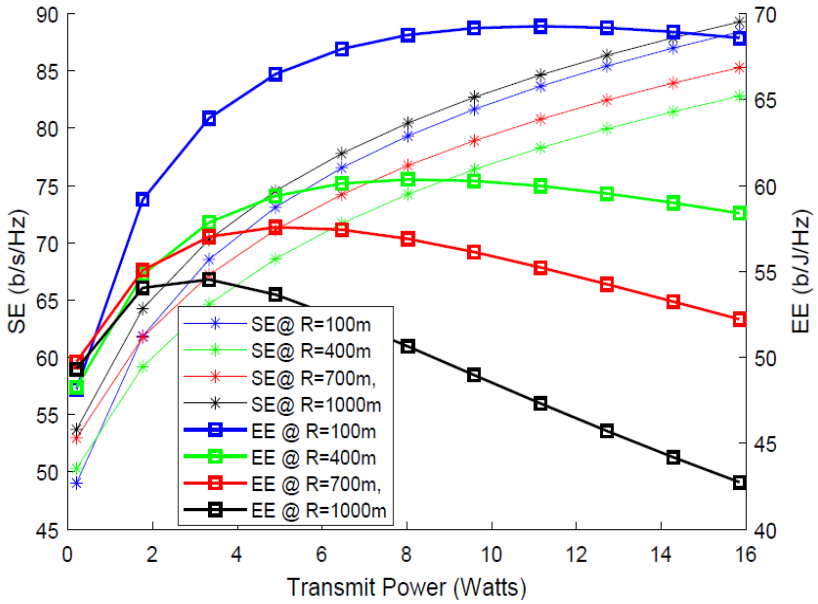

Figure 5. SE and EE at different cell radius.

In Figure 5, a further investigation of the observed EE curve reveals the effect of cell radius on its shape. For small a cell radius (e.g, 100m), the EE increases for a significant portion of the entire range of the eNodeB transmit power, only falling slightly at around the 11watts mark. Similarly, the curve for cell radius 400m and 700m shows a better performance than when the cell radius is 1000m. In the same vein the EE value is highest at the smallest cell radius. The story is however not the same for the SE curves. While SE value increases with increasing radius for R=400m, 700m and 1000m, the case of R=100m, defy the pattern. This can be explained by the fact that at lower cell radius, the interference power of the licensee is very low, thus giving more freedom for transmitting at power level closer to when the LSA spectrum is free of incumbent's ATC transmission.

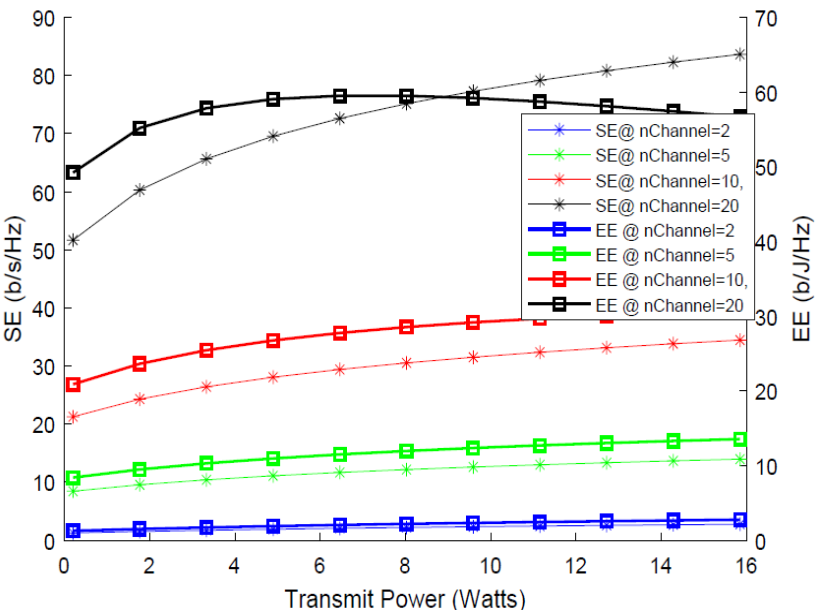

Figure 6. SE and EE for different number of UE.

Figure 6 shows the effect of number of UEs on the relationship between the system SE and EE. For two UEs, both EE and SE increases with increasing transmit power. This is a departure from the relationship depicted in Figure 4, where the EE increases initially (especially below the 3 watts transmission power mark) and then decreases as transmit power increases. The curve for five UEs, is somewhat similar. The downward slide of the EE curve starts to manifest for larger than ten UEs. This means that with the fewer number of users in the licensee cell, the network can simultaneously achieve the twin conflicting objective of improved spectrum and energy efficiency irrespective of the eNodeB transmit power configuration. This hypothesis is validated in the plots of SE against EE for different number of channels in figure 7.

As depicted in Figure7, when the number of UEs (nChannel) is 2, the graph of EE against SE is a linear curve with a positive slope/ gradient. For when nChannel is 5, the graph can still be approximated as linear, while at nChannel = 10, the curve starts exhibiting the EE downward slide observed in Figures. 4 and 6. However, when there are many users in the licensee cell, as depicted in the sub-plot for nChannel = 20, the EE stops increasing with SE at a certain point and begins to fall. At this point, the joint optimization problem, becomes a trade-off between SE and EE. Figure. 8 provides evidence/basis for manipulating the trade-off to suit a desirable preference between the two metrics given other constraints or objectives. At small cell radius, the trade-off portion of the curve is very small compared to the region of the curve where both metrics increase simultaneously. With increase in cell radius, comes extension of the trade-off portion of the EE-SE curve. As shown in the fourth sub-plot of Figure. 8, at large cell radius the downward slope of the curve begins to manifest early, hence the trade-off region dominates the EE-SE rate envelope.

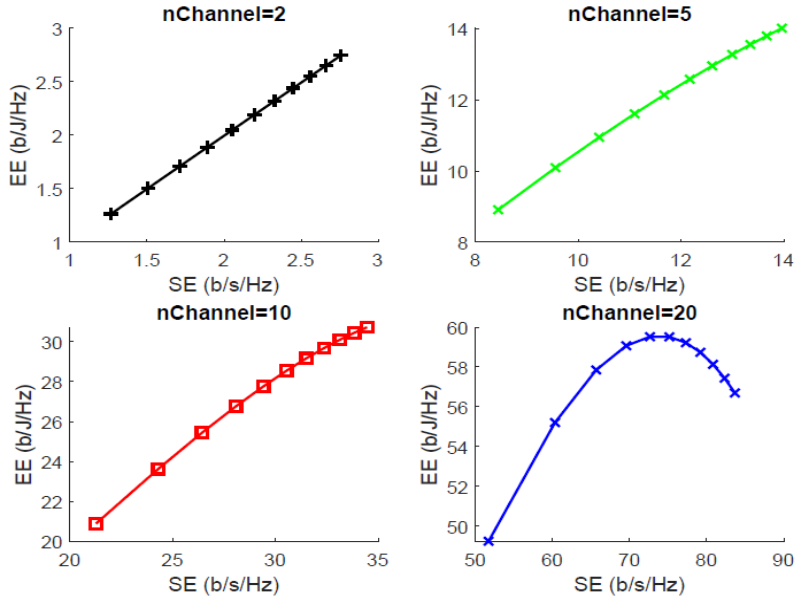

Figure 7. EE versus SE for different number of UEs.

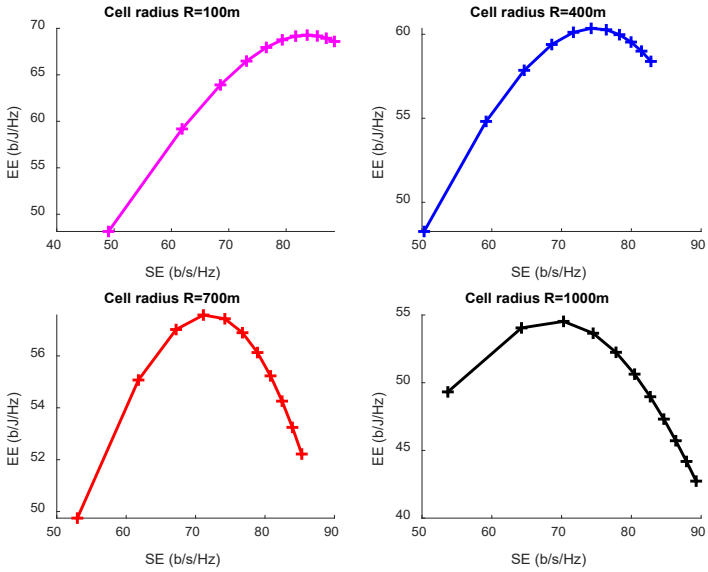

Figure 8. EE versus SE for at different cell radius.

B. Effect of Importance Weight on the SE-EE Joint Optimization

The graphs in Figure. 9 shows the extreme bounds of values of weight on objective function of our joint optimization model. At w=0, the joint optimization reduces to an energy efficiency problem. This can be seen from the shape and comparable values of the sub plots 1 and 2 in the figure. The curve in sub plot 2, is actually a plot of the systems EE against increasing transmit power. Similarly at the other extreme end of the weight parameter, i.e w=1, the optimization problem becomes an SE optimization as seen from the similarity in the sub plot 3 and the SE vs transmit power curve of sub plot 4.

Figure 10 examines how 'w' affects the SE-EE joint optimization for different number of UEs in the licensee cell. At fixed value of 'w', the magnitude of the joint SE-EE function increases with increase in the number of UEs. This is because with increasing number of users the system, SE being the summation of each channel's SE increases accordingly. This also explains the larger values of the joint SE-EE function with increasing values of 'w' especially for the case when the nChannel =20. For smaller number of UEs, the marginal difference for different values of 'w' is less obvious.

It was established in Figure. 9 that increasing 'w' increases the significance of SE while decreasing EE's significance. Thus, it can be asserted that when SE is more significant than the EE in the joint SE-EE function, larger values of the joint optimization function is obtained compared to when the situation is reversed. Furthermore as earlier established in Figure. 9, the curve for when w=0 assumes an EE shape, hence the reducing value of the function with increasing transmit power for the situation when the UE number is 20. However, for smaller user numbers, the curve tends to increase with increasing transmit power in a similar fashion to the other sub plots for values of 'w' when SE dominates the joint optimization objective function. In this regard, it can be concluded that even when EE is more significant in the joint SE-EE optimization, it is possible to achieve simultaneous increase in both EE and SE with the appropriate allocation of number of users to be served by a licensee cell.

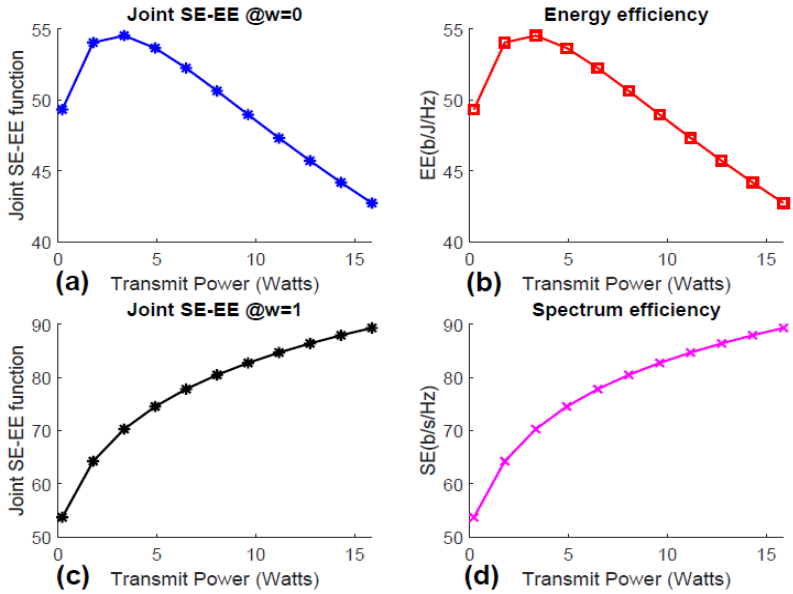

Figure 9. Upper and lower bounds of weight (w) and the joint optimization function.

Figure. 11 shows how the importance weight ('w') affects the joint SE-EE optimzation for different values of cell radius. Four different radius R=100m, 400m, 700m and 1000m were plotted. The curves show that with increasing value of 'w' the joint SE-EE function increases. However, there is a difference in the relationship between the joint SE-EE and cell radius at different values of 'w'. At w=0, there is an obvious inverse relationship while for the remaining values of w, the relationship is direct except for R=100m, which is an outlier. From this, it can be deduced that when EE dominates the SE-EE function, there is an inverse relationship between cell radius and the network efficiency (i.e the SE-EE function) and a direct relationship when SE dominates the SE-EE function.

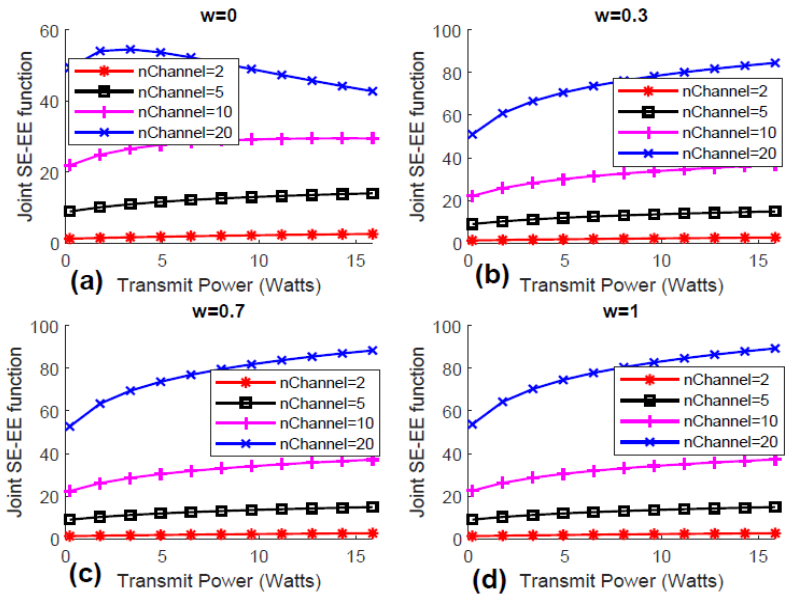

Figure 10. Effect of importance weight (w) on the number of UEs.

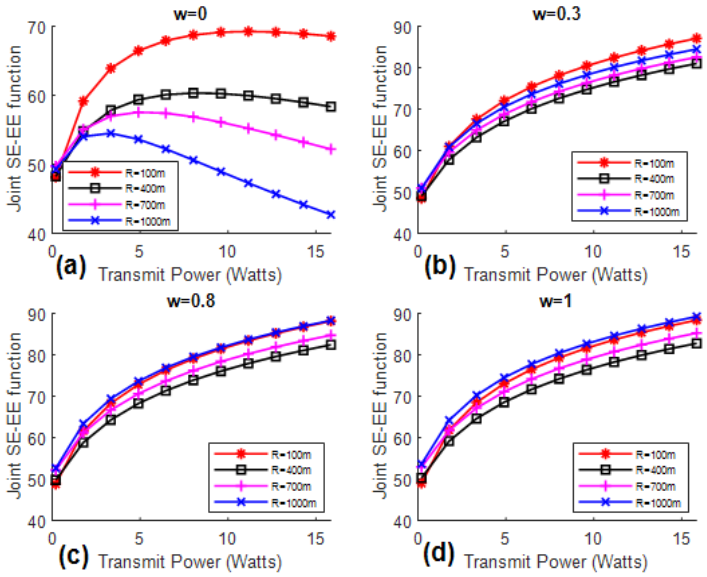

Figure 11. Effect of importance weight (w) on cell radius.

C. Effect of Circuit Power on the SE-EE Joint Optimization

The previous sub-section presents results for the proposed LSA system at constant circuit power P_{cr} of 0dB. In this sub-section, how varying the P_{cr} affects the systems performance metrics of SE and EE is investigated. In Figureure 12, a comparison of the the effect of different values of P_{cr} on the SE-EE function at different weights is done. The graphs shows that for a given w the value of the SE-EE function is increases with decrease in P_{cr}. This however is not true for $w = 1$, where the value of the SE-EE function is the same for all vaues of P_{cr}. This is because, the joint SE-EE function becomes an SE function at $w = 1$, hence P_{cr} is irrelevant. This is also reflected in the fact that as w increases the marginal difference in the values for the different P_{cr} diminishes.

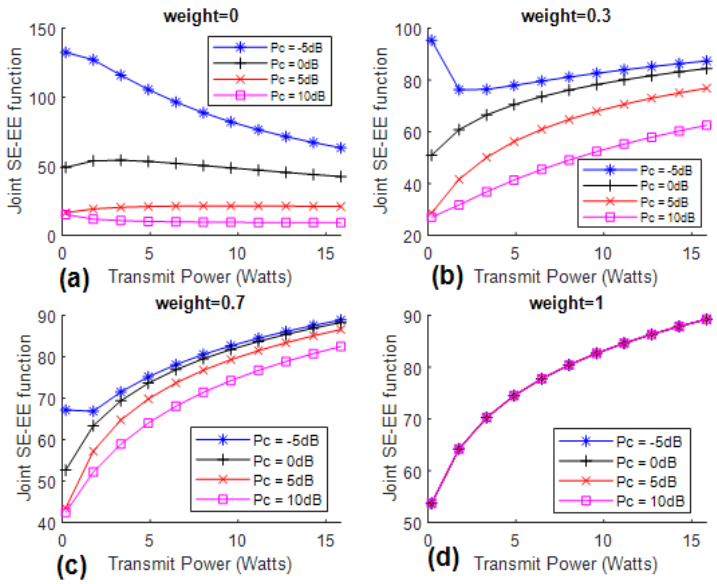

Figure 12. Effect of circuit power (P_{cr}) on importance weight.

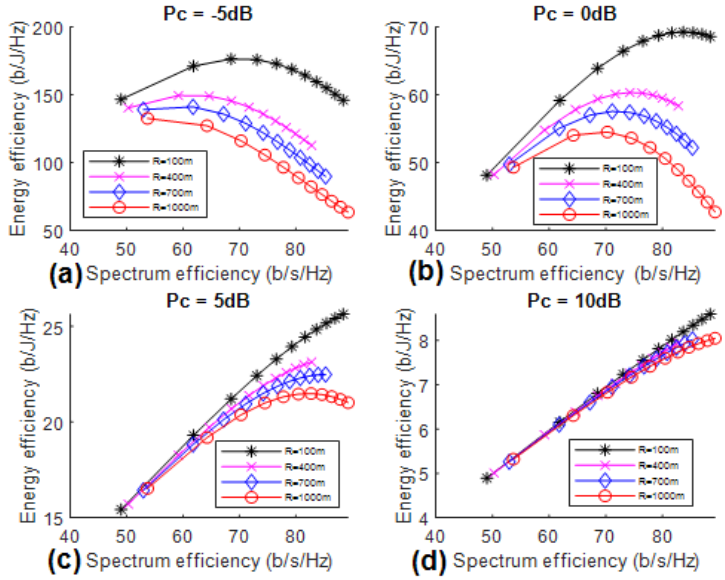

Figure 13. Effect of circuit power (P_{cr}) on cell radius.

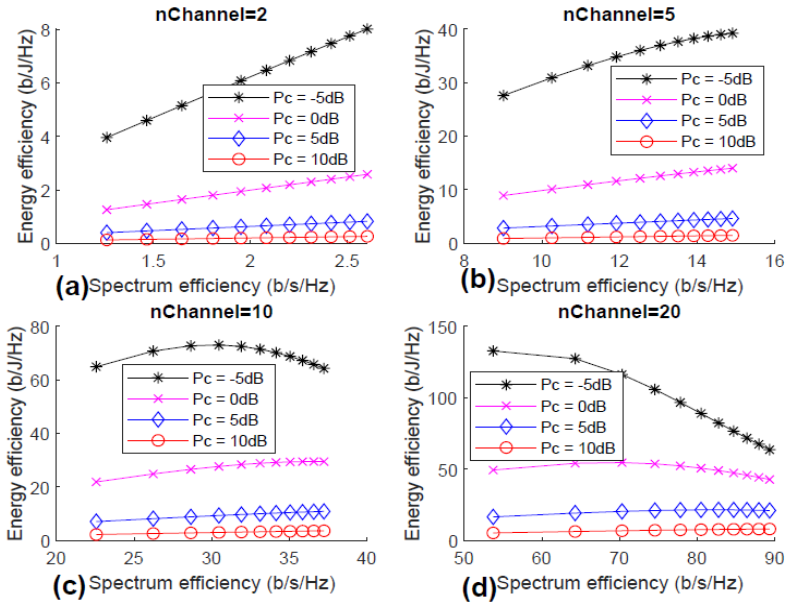

Figure 14. Effect of circuit power (P_{cr}) on user number.

Figure 13 and 14 examine the relationship between the SE and EE trade-off for different cell radius and number of users respectively while varying the P_{cr}. In Figure. 13, for all values of P_{cr}, the EE-SE trade-off, exhibits an inverse relationship with the cell radius. Furthermore with increasing value of P_{cr}, the value of the SE-EE trade-off decreases. However, the shape of the curve differs for different cell radius value as well different P_{cr} value. For R=100m, the trade-off curve increases to a maximum value then decreases for all values of P_{cr}, except for P_{cr}=10dB, where the SE-EE relationship seems to assume the shape of a monotonically increasing function. This is evidence from the fact that the region of decline of the curve decreases with increasing P_{cr} value and then culminates in an approximately monotonically increasing function of

P_{cr}=10dB. This trend is observed for other values of R. It should be noted that for R=700m and R=1000m for P_{cr}=-5dB, the trade-off assumes a monotonically decreasing function shape.

The trade-off function increases with increasing number of channels as shown in Figure. 15. For constant channel number, the trade-off decreases with increasing P_{cr}. This is so because increasing P_{cr} invariably leads to increase in total power consumption and hence decrease in EE. Noteworthy is the variation in the shape of the EE-SE curves for the different user numbers investigated in this work. At $P_{cr} \leq 0$Db, the EE-SE curve gradually changes from an increasing function to a decreasing one, while for positive values of P_{cr} the EE-SE curve is approximately linear irrespective of user number.

5. Conclusion

An extensive investigation of the system's performance (vis-a-vis EE and SE) of an LSA system especially during the period when the LSA spectrum is occupied by the incumbent was presented. Obtained results indicate that optimizing both the system's energy and spectrum efficiecy could lead to obtaining a significantly improved and efficient licensee system, while at the same time ensuring the protection of the incumbent's operation. The proposed power allocation yields muiltifold improvement in the system SE and EE especially at low transmit power. The better performance demonstrated by the system at low transmit power, on one hand, is down to the low interference power generated which combine with small cell radius and number of users, provides more degree of freedom that allows the system to operate closer to its maximum transmission power when the spectrum is idle. On the other hand, the limited transmit power regime inadvertently leads to an optimization of the systems' EE, hence more improvement of the energy efficiency with the proposed power allocation presented in this work. Furthermore, this work reveals that with the proper selection of cell radius, eNodeB transmit power and user number per cell, the LSA scheme can simultaneously achieve the twin conflicting objective of improved spectrum and energy efficiency. It is also observed that when EE dominates the weighted SE-EE function, there is an inverse relationship between cell radius and the network efficiency (i.e the SE-EE function) and a direct relationship when SE dominates the SE-EE function. Results also show that as w increases the effect of circuit power on the joint SE-EE optimization diminishes. Finally, noteworthy is the fact during this period when the spectrum is busy, the EE vs transmit power relationship which is nominally a monotonically decreasing function, first increases before a more gradual decline.

6. References

[1]. ITU-R, “IMT Vision Framework and overall objectives of the future development of IMT for 2020 and beyond (REC-M.2083-0),” *International Telecommunication Union*, September 2015.

[2]. GSMA, “Understanding 5G: Perspectives on Future Technological Advancements in Mobile,” *GSMA Intelligence Technical report*, December 2014.

[3]. B. Lannoo, C. B. Lannoo, S. Lambert, W. V. Heddeghem, M. P. (iminds, O. K. (tudelft, G. Koutitas, H. Niavis, A. S. (certh, M. Till, A. Fischer, H. D. M. (uni Passau, P. A. (ulanc, N. H. Viet, T. P. (uio, J. A. (uam, and R. T. Certh, “D8.1: Overview of ICT energy consumption,” 2012.

[4]. M. Pickavet, W. Vereecken, S. Demeyer, P. Audenaert, B. Vermeulen, C. Develder, D. Colle, B. Dhoedt, and P. Demeester, “Worldwide energy needs for ICT: The rise of power-aware networking,” in 2008 2nd *International Symposium on Advanced Networks and Telecommunication Systems*, Dec 2008, pp. 1–3.

[5]. Smart2020, “Enabling the low Carbon Economy in the Information age,” The Climate Group, London, U.K., Tech. Rep., 2008.

[6]. C. Hepburn and N. Stern, “A new global deal on climate change,” Oxford Review of Economic Policy, vol. 24, no. 2, pp. 369–395, Apr 2008.

[7]. Z. Hasan, H. Boostanimehr, and V. K. Bhargava, "Green cellular networks: A survey, some research issues and challenges," *IEEE Communications Surveys Tutorials*, vol. 13, no. 4, pp. 524–540, Fourth 2011.

[8]. K. Lahiri, A. Raghunathan, S. Dey, and D. Panigrahi, "Battery-driven system design: a new frontier in low power design," in Proceedings of ASP-DAC/VLSI Design 2002. 7th *Asia and South Pacific Design Automation Conference and 15h International Conference on VLSI Design*, Jan 2002, pp. 261–267.

[9]. "Ericsson Mobility Report," June 2018.

[10]. "Ericsson Mobility Report," November 2018.

[11]. Cisco, "Cisco Visual Networking Index: Forecast and Methodology, 2016 - 2021," "White Paper", Tech. Rep., June, 2017.

[12]. ITU-R, "IMT traffic estimates for the years 2020 to 2030-Report ITU-R M.2370-0," *International Telecommunication Union*, July 2015.

[13]. Y. Chen, S. Zhang, S. Xu, and G. Y. Li, "Fundamental Trade-offs on Green Wireless Networks," *IEEE Communications Magazine*, vol. 49, no. 6, pp. 30–37, June 2011.

[14]. "ECC Report 205: Licensed Shared Access (LSA), CEPT Working Group Frequency Management," February 2014.

[15]. ETSI, "TR 103 113 - V1.1.1 - Electromagnetic compatibility and Radio spectrum Matters (ERM); System Reference document (SRdoc); Mobile broadband services in the 2300 MHz - 2400 MHz frequency band under Licensed Shared Access regime..

[16]. P. Masek, E. Mokrov, A. Pyattaev, K. Zeman, A. Ponomarenko-Timofeev, A. Samuylov, E. Sopin, J. Hosek, I. A. Gudkova, S. Andreev, V. Novotny, Y. Koucheryavy, and K. Samouylov, "Experimental Evaluation of Dynamic Licensed Shared Access Operation in Live 3GPP LTE System," in 2016 *IEEE Global Communications Conference (GLOBECOM)*, Dec 2016, pp. 1–6.

[17]. M. Palola, M. Matinmikko, J. Prokkola, M. Mustonen, M. Heikkil, T. Kippola, S. Yrjl, V. Hartikainen, L. Tudose, A. Kivinen, J. Paavola, and K. Heiska, "Live field trial of Licensed Shared Access (LSA) concept using LTE network in 2.3 GHz band," in 2014 *IEEE International Symposium on Dynamic Spectrum Access Networks (DYSPAN)*, April 2014, pp. 38–47.

[18]. M. Palola, M. Matinmikko, J. Prokkola, M. Mustonen, M. Heikkil,T. Kippola, S. Yrjl, V. Hartikainen, L. Tudose, A. Kivinen, J. Paavola, K. Heiska, T. Hnninen, and J. Okkonen, "Description of Finnish Licensed Shared Access (LSA) Field Trial Using TD-LTE in 2.3 GHz Band," in 2014 *IEEE International Symposium on Dynamic Spectrum Access Networks (DYSPAN)*, 2014, pp. 374–375.

[19]. M. Palolo, T. Rautio, M. Matinmikko, J. Prokkola, M. Mustonen, M. Heikkil, T. Kippola, S. Yrjl, V. Hartikainen, L. Tudose, A. Kivinen, J. Paavola, J. Okkonen, M. Mkelinen, T. Hnninen, and H. Kokkinen, "Licensed Shared Access (LSA) trial demonstration using real LTE network," in 2014 9th *International Conference on Cognitive Radio Oriented Wireless Networks and Communications (CROWNCOM)*, June 2014, pp. 498–502.

[20]. M. Matinmikko, M. Palola, M. Mustonen, T. Rautio, M. Heikkil, T. Kippola, S. Yrjl, V. Hartikainen, L. Tudose, A. Kivinen, H. Kokkinen, and M. Mkelinen, "Field trial of Licensed Shared Access (LSA) with enhanced LTE resource optimization and Incumbent protection," in 2015 *IEEE International Symposium on Dynamic Spectrum Access Networks (DySPAN)*, Sept 2015, pp. 263–264.

[21]. J. Kalliovaara, T. Jokela, R. Ekman, J. Hallio, M. Jakobsson, T. Kippola, and M. Matinmikko, "Interference measurements for Licensed Shared Access (LSA) between LTE and wireless cameras in 2.3 GHz band," in 2015 *IEEE International Symposium on Dynamic Spectrum Access Networks (DySPAN)*, Sept 2015, pp. 123–129.

[22]. D. Guiducci, C. Carciofi, V. Petrini, S. Pompei, J. Llorente, V. Ferrer, J. Costa-Requena, E. Spina, G. D. Sipio, D. Massimi, D. Spoto, F. Amerighi, T. Magliocca, H. Kokkinen, P. Chawdhry, L. Ardito, S. Yrjola, V. Hartikainen, L. Tudose, P. Muller, M. Gianesin, F. Grazioli, and D. Caggiati, "Sharing under Licensed Shared Access in a live LTE network

in the 2.32.4 GHz band end-to-end architecture and compliance results," in 2017 *IEEE International Symposium on Dynamic Spectrum Access Networks (DySPAN)*, March 2017, pp. 1–10.

[23]. I. Gudkova, K. Samouylov, D. Ostrikova, E. Mokrov, A. Ponomarenko-Timofeev, S. Andreev, and Y. Koucheryavy, "Service failure and interruption probability analysis for licensed shared access regulatory framework," in 2015 7th *International Congress on Ultra Modern Telecommunications and Control Systems and Workshops (ICUMT)*, Oct 2015, pp. 123–131.

[24]. V. Y. Borodakiy, K. E. Samouylov, I. A. Gudkova, D. Y. Ostrikova, A. A. Ponomarenko-Timofeev, A. M. Turlikov, and S. D. Andreev, "Modeling Unreliable LSA Operation in 3GPP LTE Cellular networks," in 2014 6th *International Congress on Ultra Modern Telecommunications and Control Systems and Workshops (ICUMT)*, Oct 2014, pp. 390–396.

[25]. I. Gudkova, A. Korotysheva, A. Zeifman, G. Shilova, V. Korolev, S. Shorgin, and R. Razumchik, "Modeling and analyzing licensed shared access operation for 5g network as an inhomogeneous queue with catastrophes," in 2016 8th *International Congress on Ultra Modern Telecommunications and Control Systems and Workshops (ICUMT)*, Oct 2016, pp. 282–287.

[26]. I. Gudkova, E. Markova, P. Masek, S. Andreev, J. Hosek, N. Yarkina, K. Samouylov, and Y. Koucheryavy, "Modeling the Utilization of a Multi-tenant band in 3GPP LTE system with Licensed Shared Access," in 2016 8th *International Congress on Ultra Modern Telecommunications and Control Systems and Workshops (ICUMT)*, Oct 2016, pp. 119–123.

[27]. E. Markova, I. Gudkova, A. Ometov, I. Dzantiev, S. Andreev, Y. Koucheryavy, and K. Samouylov, "Flexible Spectrum Management in a Smart City Within Licensed Shared Access Framework," *IEEE Access*, vol. 5, pp. 22 252–22 261, 2017.

[28]. K. Laehetkangas, H. Saarnisaari, and A. Hulkkonen, "Licensed Shared Access System Development for Public Safety," in European Wireless 2016; 22th *European Wireless Conference*, May 2016, pp. 1–6.

[29]. A. Ponomarenko-Timofeev, A. Pyattaev, S. Andreev, Y. Koucheryavy, M. Mueck, and I. Karls, "Highly Dynamic Spectrum Management within Licensed Shared Access regulatory framework," *IEEE Communications Magazine*, vol. 54, no. 3, pp. 100–109, March 2016.

[30]. E. Mokrov, A. Ponomarenko-Timofeev, I. Gudkova, P. Masek, J. Hosek, S. Andreev, Y. Koucheryavy, and Y. Gaidamaka, "Transmit Power Reduction for a Typical Cell With Licensed Shared Access Capabilities," *IEEE Transactions on Vehicular Technology*, vol. 67, no. 6, pp. 5505– 5509, June 2018.

[31]. M. Hafeez and J. M. H. Elmirghani, "Green licensed-shared access," *IEEE Journal on Selected Areas in Communications*, vol. 33, no. 12, pp. 2579–2595, Dec 2015.

[32]. Deloitte, "The-Impacts of Licensed Shared-Use-of-Spectrum, report for GSM association," January 2014.

[33]. M. Haenggi, Stochastic Geometry for Wireless Networks, 1st ed. New York, NY, USA: Cambridge University Press, 2012.

[34]. E. S. Sousa and J. A. Silvester, "Optimum Transmission Ranges in a Direct-sequence spread-spectrum Multihop Packet Radio Network," *IEEE Journal on Selected Areas in Communications*, vol. 8, no. 5, pp. 762–771, Jun 1990.

[35]. M. Haenggi and R. K. Ganti, "Interference in Large Wireless Networks," Foundations and Trends in Networking, vol. 3, no. 2, pp. 127–248, 2009. [Online]. Available: http://dx.doi.org/10.1561/1300000015

[36]. R. T. Marler and J. S. Arora, "Survey of multi-objective optimization methods for engineering," Struct. Multidisciplinary Optim, vol. 26, no. 6, pp. 369–395, Apr 2004.

[37]. S. Schaible, "Minimization of Ratios," Journal of Optimization Theory and Applications, vol. 19, no. 2, pp. 369–395, Jun 1976.

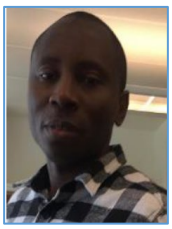

Samuel O. Onidare received B.Tech degree in Electronic and Electrical Engineering from Ladoke Akintola University of Technology, Ogbomoso, Oyo State, Nigeria in 2000, and MSc. in Electrical Engineering with emphasis on Telecommunication from Blekinge Teckniska Hogskola, Karlskrona, Blekinge, Sweden in 2010. He obtained Ph.D. in Communication in 2021 from the School of Computing and Communication Systems at Lancaster University, United Kingdom. His research interest includes mobile wireless communication and networks with an emphasis on spectrum sharing, green communications, and wireless resource allocation and optimization.

Osuolale A. Tiamiyu A computer network and telecommunications specialist; with good multinational working experience and achievements in companies like Motorola, EXQU Ltd Nigeria, and several academic institutions. He holds a Ph.D. in "Systems, Networks and Telecommunication Devices" (St. Petersburg), also MSc & BSc degrees (Moscow) in Engineering Science "Informatics and Computer Engineering", specializing in Computer Networks & Telecommunications. He has already, published many journal articles and he has a patent right (RU Patent № 150245) on a Trusted Routing Mechanism. His research interest is in Computing, Computer Networks, and Network Security.

Quadri R. Adebowale is a young academic researcher from the prestigious University of Ilorin, Ilorin, Nigeria. I had a B.Sc. Telecommunication Science at University of Ilorin, Nigeria, and bagged a master's degree in Telecommunication Science with a focus on wireless and cellular communication, University of Ilorin, graduating with distinction. I am currently undergoing my Ph.D. study at Ohio University, United States of America. My research interest revolves around Routing techniques in delay tolerant networks, wireless radio propagation in lunar surface, machine learning, deep learning, software-defined wireless sensor networks, heterogeneous networks, and Networking. I have published in various local, National, and international journals.

Oluwaseun T. Ajayi received a B.Sc. degree in Telecommunication Science from the University of Ilorin, Nigeria, in 2018. He is currently working toward a Ph.D. degree with Illinois Institute of Technology. His research interests include machine learning in wireless networks, information freshness optimization, and vehicular communications.

Kazeem B. Adewole is a Research Assistant at Kent State University in Kent, OH (USA). Prior to this, he was affiliated with the Computer Science Department of the University of Ibadan of Nigeria, where he participated in conducting research that focuses on computer networks and cybersecurity as well as research that proposes the use of an artificial intelligence model to mitigate the effect of zero-day attacks in IoT devices. His additional interests include artificial intelligence, big data with a concentration on the Internet of

Things (IoT), and blockchain technology. He is concurrently working on debunking the misconception of central bank digital currency (CBDC) and designing a sophisticated AI model to enhance generative adversarial networks using a deep learning approach. Coupled with his research experience, Babatunde has many multinational working experiences and achievements in companies like Zenith Bank Plc, Viable Technologies Limited, Greensprings School, World Health Organization of Nigeria, and now a proud founder of Teleminer Concept Global Enterprise. He received his Bachelor of Science Degree in Telecommunication Science,
a Master of Science Degree in Computer Science, and a Master of Business Administration Degree all at the University of Ilorin of Nigeria. He is currently obtaining his Ph.D. in Computer Science with a concentration in Cybersecurity, at Kent State University. In addition to that, Babatunde has been published in the International Journal of Advancements in Research and Technology and is a member of the Association of Computing Machinery (ACM) and the Institute of Electrical Electronics Engineering (IEEE).

Adeseko A. Ayeni holds a PhD in Electrical Engineering. He has industrial experience in telecommunications, having worked for NITEL and for ELTEC. He joined academics and rose gradually to become a professor, having mentored younger scholars and researchers. His research area is wireless communication, radio path profiling, white space detection & radio spectrum sharing. He is a member of IEEE, NSE and he is COREN registered.